Oceanography Surrounding Krakatau Volcano
in the Sunda Strait, Indonesia

By R. Dwi Susanto, Zexun Wei, T. Rameyo Adi,
Quanan Zheng, Guohong Fang, Bin Fan,
Agus Supangat, Teguh Agustiadi, Shujiang Li,
Mukti Trenggono, and Agus Setiawan

ABSTRACT. Seasonal variability of water properties obtained from conductivity-temperature-depth casts from 2008 to 2015 and current velocities obtained from moorings deployed from 2008 to 2009 show that the Sunda Strait plays dual roles in water exchange between the Pacific and Indian Oceans. The Sunda Strait current velocity is strongly affected by seasonal monsoon winds. During the boreal winter monsoon, northwesterly winds to the north and south of Java draw waters from the Indian Ocean into the Java Sea, and at the same time, the Java Sea receives an influx of low-salinity water from the South China Sea. Summation of these waters would reduce the main Indonesian Throughflow transport in the Makassar Strait. Conditions are reversed during the summer monsoon: higher-temperature, lower-salinity, and lower-density waters from the Java Sea are exported to the Indian Ocean through the Sunda Strait, enhancing Indonesian Throughflow transport from the Pacific into the Indian Ocean. Variations in temperature, salinity, and density are greater during the boreal summer than those observed during the winter monsoon. Kelvin-wave-like signals have been observed in the velocity time series data; however, further investigation in this region is needed to confirm the possibility of Kelvin waves entering the Sunda Strait.

INTRODUCTION

The Sunda Strait, centered at 6.0°S, 105.0°E, separates the Indonesian islands of Java and Sumatra, and connects the Java Sea and the Indian Ocean (Figure 1). The strait is also the westernmost exit for Pacific Ocean and Indonesian Seas waters entering the Indian Ocean along the Lesser Sunda Islands from Sumatra to Timor. The Indonesian Throughflow (ITF), which winds its way through the complex coastlines and narrow passages of the Indonesian Seas, is a major oceanic pathway for Pacific to Indian inter-ocean exchange and for transferring climatic signals as part of the global ocean circulation (Figure 1a). The ITF is driven by regional and remote forcings from the Pacific and the Indian Oceans, and is modulated by various ocean-atmospheric forcings that vary from intraseasonal to interannual time scales. Trade winds push tropical Pacific warm water westward, generating a western Pacific warm pool and higher sea levels, and setting up a pressure gradient between the Pacific and Indian Oceans (Wyrtki, 1987). The ITF's total volume transport and heat and freshwater fluxes are known to impact both the Pacific and Indian Oceans. In addition, the ITF modulates climate variability by altering air-sea exchange, sea surface temperature, and regional precipitation patterns over many time scales, and it possibly influences the El Niño-Southern Oscillation (ENSO) and Asian-Australian monsoon climate phenomena (e.g., Godfrey, 1996; Schneider, 1998; Bryden and Imawaki, 2001; T. Lee et al., 2002; Aldrian and Susanto, 2003; T. Lee and McPhaden, 2008; Tokinaga et al., 2012; Sprintall et al., 2014). In the last two decades, ITF transport increased significantly (Sprintall and Revelard, 2014; Susanto and Song, 2015), increasing the Indian Ocean heat content, which may have strong impacts on global climate (S-K. Lee et al., 2015; Reed, 2015).

The main ITF inflow pathways are the central passage of Makassar Strait (~80%), an eastern route through Lifamatola Passage/Seram Sea, and a western route via the South China Sea. Meanwhile, the main exit passages are the Lombok and Ombai Straits and Timor Passage. The inflow and outflow ITF transport is nearly closed but not fully balanced (Gordon et al., 2010). Figure 1a shows the ITF pathways with their annual mean transports and standard deviations in Sv (1 Sv = 1×10^6 m s^{-1}; Gordon et al., 2008, 2010; Sprintall et al., 2009; van Aken et al., 2009; Fang et al., 2010; Susanto et al., 2012, 2013; Wei et al., 2015). Note that the number in Lifamatola Passage represents the deep transport only (below 1,250 m). The plus and minus signs in Karimata Strait represent seasonal reversal transports to/from the South China Sea from/to the Java Sea: negative during the boreal winter monsoon and positive during the boreal summer monsoon. In this region, the boreal winter monsoon occurs from November to March, while the summer monsoon occurs from May to September. April and October are the monsoon transition months (Aldrian and Susanto, 2003). The main ITF from the Pacific Ocean through the Makassar Strait is concentrated in the upper 650 m (controlled by the depth of Dewakang Sill located at the southern end of the strait), with a maximum velocity within the thermocline at 120–150 m depth (Susanto et al., 2012). The upper layer varies with the monsoon, and is affected by freshwater from the Java Sea that originates in the South China Sea (Gordon et al., 2003; Fang et al., 2009; Susanto et al., 2012, 2013) and the Sulu Sea (Gordon et al., 2012). Previous investigators suggest that during the boreal winter monsoon, Java Sea low-salinity water from the South China Sea accumulates in the southern Makassar Strait, controlling the vertical structure and stratification of the main ITF in this region before its waters exit into the Indian Ocean (Gordon et al., 2003, 2012; Qu et al., 2006; Fang et al., 2009; Tozuka et al., 2009; Susanto et al., 2012, 2013).

The Sunda Strait connects the Indian Ocean in the south (>5,000 m depth; 82 km width) to the Java Sea in the north (narrowest width of 18 km). The small Sangeang Island splits the northern end of the Sunda Strait into two channels: the western channel with 98 m water depth and the eastern channel with 70 m water depth. The width of the Sunda Strait is comparable to that of the southern end of the Lombok Strait (east of Nusa Penida Island), which is 20 km wide and has a maximum sill depth of ~350 m (Murray and Arief, 1988). Because the Sunda Strait directly connects the Java Sea to the Indian Ocean, it is expected that the Sunda Strait plays a role in freshwater exchange between the Pacific and Indian Oceans. We are particularly interested in learning how Sunda Strait flow influences the Java Sea. Is it in sync or out of

phase with the seasonal flow from the South China Sea through the Karimata Strait into the Java Sea? If it is in sync, the Karimata and Sunda Straits' low-salinity waters that flow into the Java Sea would reduce the main ITF flow in the Makassar Strait.

The Sunda Strait provides the only commercial shipping lane from/to Australia and Singapore, a major commercial shipping hub for the Southeast Asia region. Historically, the strait provided direct passage from the Indian Ocean to Jakarta, the capital of Indonesia, so that it was the center of a major World War II naval battle for US, Japanese, and Dutch warships. Krakatau Volcano, which erupted August 26–28, 1883, killing more than 30,000 people, lies in the middle of the strait. The eruption blasts were heard nearly 3,000 miles away, and the resulting ash affected the whole globe and cooled the atmosphere by a couple of degrees for more than 15 years (Simkin and Fiske, 1983). The volcano largely disappeared during the eruption. Now, an active growing volcano "Anak Krakatau," located adjacent to the Krakatau crater, adds to the complexity of the rough topography in the Sunda Strait (Figure 1c). It is not known whether geothermal processes associated with the older Krakatau crater or the volcanically active Anak Krakatau influence Sunda Strait water characteristics and circulation.

Since the Sunda Strait provides the first water gap along the Indonesian Archipelago from Sumatra in the west to Timor in the east, the question of whether coastally trapped long waves (Kelvin waves) could enter the Sunda Strait also remains unanswered. During the monsoon transition in April and October, there is an anomalous westerly wind burst in the central equatorial Indian Ocean known as the "Wyrtki jet" (Wyrtki, 1973) that generates Kelvin waves that propagate eastward along the equator in the Indian Ocean. When approaching the coast of Sumatra, the waves split into two parts, with one part propagating northward and the other southward as coastally trapped Kelvin waves. Previous investigators (e.g., Sprintall et al., 2000; Susanto et al., 2000, 2012; Syamsudin et al., 2004; Iskandar et al., 2005; Shinoda et al., 2012) found that Kelvin waves propagate along the southern coast of Sumatra and Java and all the way along the series of the Lesser Sunda Island Chain to Timor. The waves also enter the Lombok Strait and influence the main ITF in the Lombok and Makassar Straits (Figure 1).

In addition, boreal summer upwelling (low sea level and low sea surface temperature) along the southern Java-Sumatra coast is induced by seasonal winds and influenced by the interannual variability associated with ENSO and the Indian Ocean Dipole (IOD; Susanto et al., 2001). The IOD is an interannual phenomenon associated with sea surface temperature (SST) differences between the tropical western Indian Ocean (10°S to 10°N and 50°E to 70°E) and the tropical southeastern Indian Ocean (10°S to the equator and 90°E to 110°E, inclusive
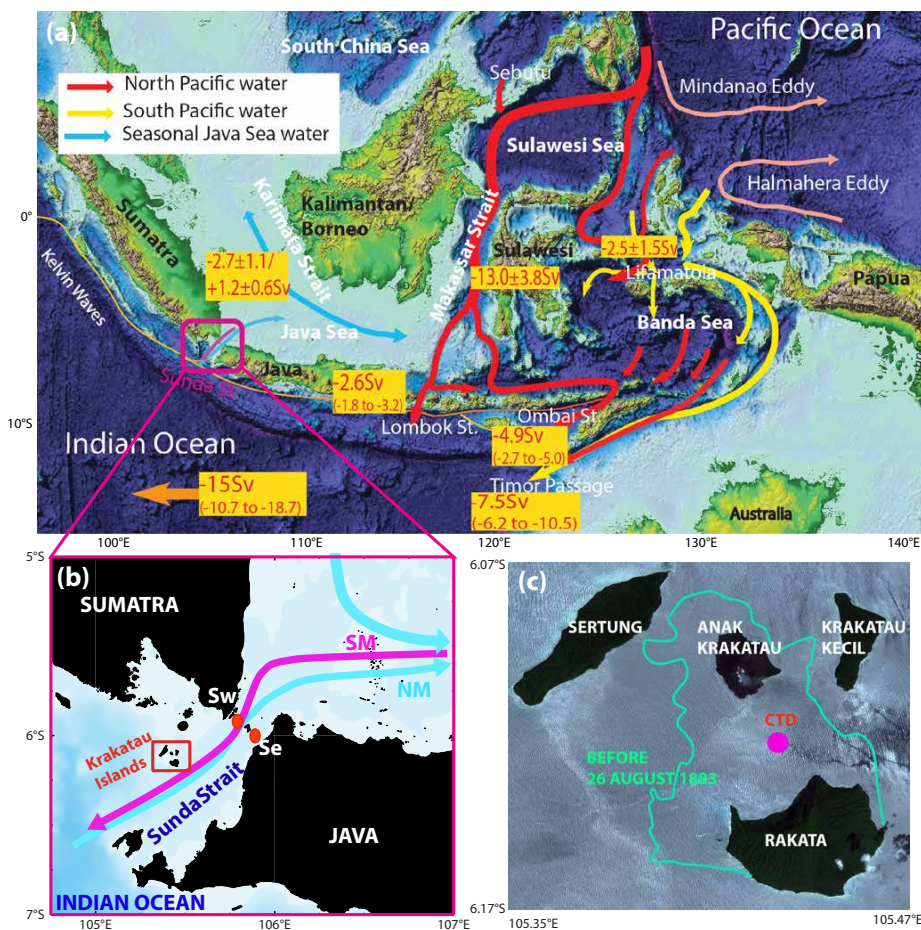

FIGURE 1. (a) The Indonesian Throughflow pathways and their annual volume transport (1 Sv = 10^6 m^3 s^{-1}). Inflow passages: Makassar Strait, Lifamatola Passage (below 1,250 m only), and Karimata Strait. Outflow passages: Lombok Strait, Ombai Strait, and Timor Passage. Negative values denote transport toward the Indian Ocean (Fang et al., 2010; Gordon et al., 2008, 2010; Sprintall et al., 2009; van Aken et al., 2009; Susanto et al., 2012, 2013; Susanto and Song, 2015; Wei et al., 2015). (b) Map of the Sunda Strait between the islands of Java and Sumatra, with seasonally reversed flows indicated for the boreal winter monsoon (northwest monsoon/NM, drawn in cyan) and the boreal summer monsoon (southeast monsoon/SM, drawn in purple). Two moorings are located at the northern outlet of the Sunda Strait (red dots labeled Sw for Sunda West and Se for Sunda East). The Krakatau Islands lie in the middle of the strait (red box). (c) Map of the Krakatau Islands from a Landsat image taken on December 10, 2014 (adapted from the Digital globe). Five conductivity-temperature-depth (CTD) stations are clustered where the original submerged crater of Krakatau Volcano was located before the eruption of August 26–28, 1883 (large pink dot). The green line shows the boundaries of Krakatau Volcano before 1883 (Simkin and Fiske, 1983).

of the southern end of the Sunda Strait); the gradient between the two is known as the Dipole Mode Index (DMI; Saji et al., 1999). A positive DMI indicates the west SST minus the east SST is positive, and vice versa. Some scientists believe IOD is dependent on ENSO, while other scientists believe that IOD is independent of ENSO; such an analysis is beyond the scope of this paper. It is still an open question as to whether the interannual ENSO and IOD phenomena may impact Sunda Strait dynamics.

Moreover, an intraseasonal phenomenon with a period between 40 and 50 days known as Madden Julian Oscillation (MJO; Madden and Julian, 1994) propagates eastward along the equatorial Indian Ocean, which adds more complexity to Indonesian Seas dynamics. It is unknown how (if at all) MJO may affect Sunda Strait dynamics. Hence, it is hypothesized that Sunda Strait dynamics are affected by both its complex coastline topography and its bathymetry, and also by intraseasonal to interannual variability associated with MJO, the monsoon, IOD, and ENSO. Despite all of these influences, the Sunda Strait remains relatively unknown to the ocean science community due to lack of observational data. This article aims to present oceanographic conditions (variability of water characteristics and ocean current velocities) in the Sunda Strait based on new data collected by several cruises led by a multinational team of scientists from 2008 to 2015.

FIELD MEASUREMENTS

In November 2008, scientists from Balitbang KP (Indonesia), the First Institute of Oceanography (China), and Columbia University and the University of Maryland (United States) collaborated to deploy two trawl-resistant, bottom-mounted acoustic Doppler current profilers (ADCP) in the narrow passage of the northern Sunda Strait to collect full-depth velocity profiles—Sunda West (designated Sw, at 98 m depth) and Sunda East (Se, at 34 m depth; Figure 1b). In addition, 76 conductivity-temperature-depth

(CTD) casts (37 during the summer monsoon and 39 during the winter monsoon) were collected from R/V *Baruna Jaya VIII* during the mooring deployment and recovery cruises as well as in subsequent years. All CTD measurements were taken at full depth except where water depths were greater than 1,000 m. In those cases, the CTD measurements were collected to 1,000 m depth only. On every cruise, we eagerly obtained CTD casts from the original Krakatau Volcano crater; however, it was too dangerous to collect these measurements when Anak Krakatau Volcano was active. Despite a series of eruptions from October 25, 2010, to March 2011, from August 2011 to October 2012, and most recently from April 22 to May 25, 2015 (Global Volcanism Program, Smithsonian Institution, http://volcano.

si.edu/volcano.cfm?vn=262000), we were able to obtain five CTD casts (two during the summer monsoon and three during the early winter monsoon) from inside the original Krakatau crater. We derive the seasonal variability of water properties in the Sunda Strait from these CTD data and discuss the results in the next section.

WATER PROPERTIES IN THE SUNDA STRAIT

The CTD data set obtained from above the original, submerged Krakatau crater (Figure 1c, pink dot in right panel) covers both southeast and northwest monsoons. Figure 2 shows water properties (temperature, salinity, and density) in the original crater during (a) the early boreal winter (northwest monsoon), and (b) the boreal summer (southeast monsoon).
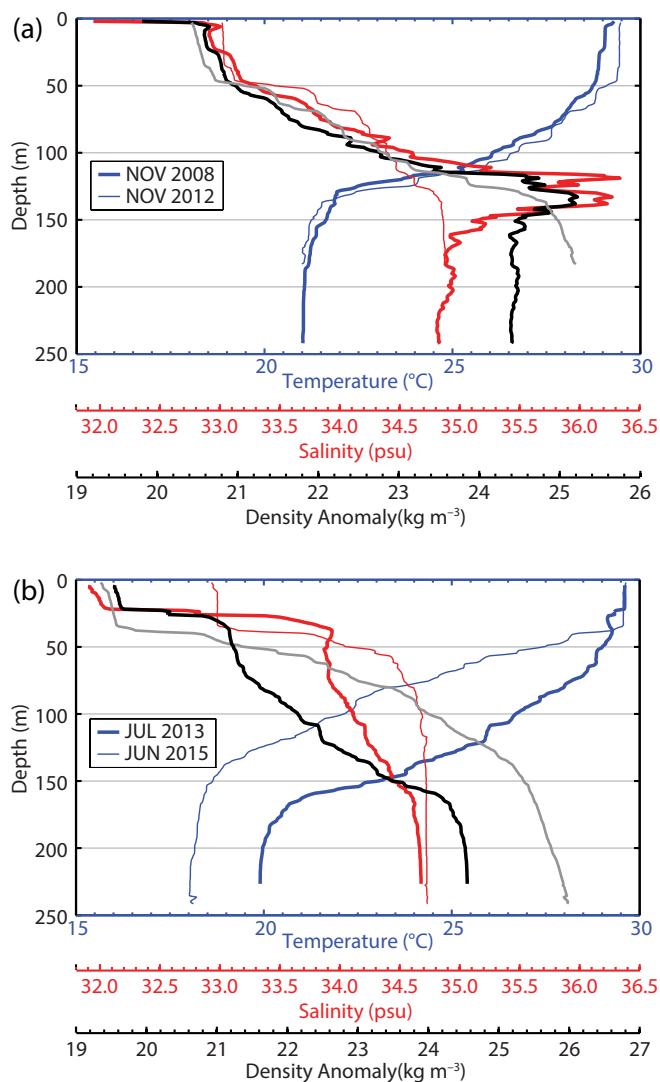

FIGURE 2. Temperature, salinity, and density anomaly [(σ_o) profiles; σ_o is density $-1,000$ kg m^{-3}] at the location of the original Krakatau Volcano crater during (a) the early boreal winter monsoon in November 2008 and 2012, and (b) the boreal summer monsoon in July 2013 and June 2015. No significant temperature increase in the bottom of the crater was observed (except for a minor increase in June 2015), indicating that despite the volcanic activity of Anak Krakatau, there are no signs of bottom geothermal plumes in the original crater of Krakatau.

Large variations in water properties are seen not only between monsoon seasons but also within each monsoon. The mixed layer depth is deeper during the winter monsoon (~50 m) than during the summer monsoon (~30 m). Temperature shows less variation compared to the salinity and density below 140 m. Below the mixed layer depth (between 50 m and 150 m water depth), temperature, salinity, and density differences between the summer monsoons of 2013 and 2015 are ~2°C, ~0.5 psu, and 1.8 kg m^{-3}, respectively. Surprisingly, there was a strong salinity maximum of 36.2 psu and a density maximum of 1,026.5 kg m^{-3} between 120 m and 140 m depth in November 2008, but they were not observed in November 2012. The salinity maximum observed in November 2008 was puzzling, because CTD data collected during the same cruise at both the entrance/exit passages on the northeastern side (Sunda Strait) and the southern side (Indian Ocean) of the original Krakatau crater did not show any salinity maximum at this depth (Figure 3). We speculate that the salinity and density maxima may be associated with the eruption of Anak Krakatau on October 23, 2007 (http://volcano.si.edu). In addition, given that Anak Krakatau is active, it is possible that geothermal plumes could emanate from the bottom of the original Krakatau crater or from Anak Krakatau. However, we do not see any significant temperature increase at the bottom of the original crater (Figure 2) that would suggest presence of geothermal plumes, although there is a small increase of bottom temperature observed in June 2015.

Figure 4 shows the horizontal distributions of temperature, salinity, and potential density anomaly (σ_0) averaged in the top 20 m of the water column, derived from 2008 to 2015 cruise observations.

Because Krakatau, which is located in the middle of the strait, is connected to the island of Sumatra on the west by series of small island chains and very shallow passages, the main channel flow occurs to the east of the volcano. Figure 5 shows the vertical distributions of temperature, salinity, and density from the Indian Ocean side (I) to the Java Sea side (J) in the area bounded by the purple box in the right panel of Figure 4c. During the boreal summer, the upper layer of the Sunda Strait fills with fresher, lower-density water from the Java Sea, while during the boreal winter, it fills with colder, saltier, higher-density water from the Indian Ocean. It is important to note that even though the salinity in the upper layer of Sunda Strait is higher (maximum 33.5 psu) during winter than in summer, this salinity value is still lower/fresher than average ocean salinity water (35 psu). Because the CTD casts were collected during the early winter monsoon, it is expected that during the peak period of the winter monsoon (December to February), the data would show a spatial distribution of Indian Ocean water intrusion into the Java Sea, as observed by the mooring velocity time series to be discussed in the next section.

SEASONAL VARIABILITY OF CURRENT VELOCITIES

The ADCP data from the Sunda East mooring cover a period from November 9, 2008, to October 20, 2009, while Sunda West data cover November 9, 2008, to July 22, 2009. Both ADCPs have been configured for a 20-minute time interval and a 2 m vertical bin. Hourly mean currents from the bottom to the surface were calculated from the ADCP bin time series. To avoid problems caused by surface reflection contamination of the ADCP data, the six uppermost layers are replaced with the values linearly extrapolated from the seventh and ninth layers, based on an assumption of constant shear (Susanto et al., 2012).

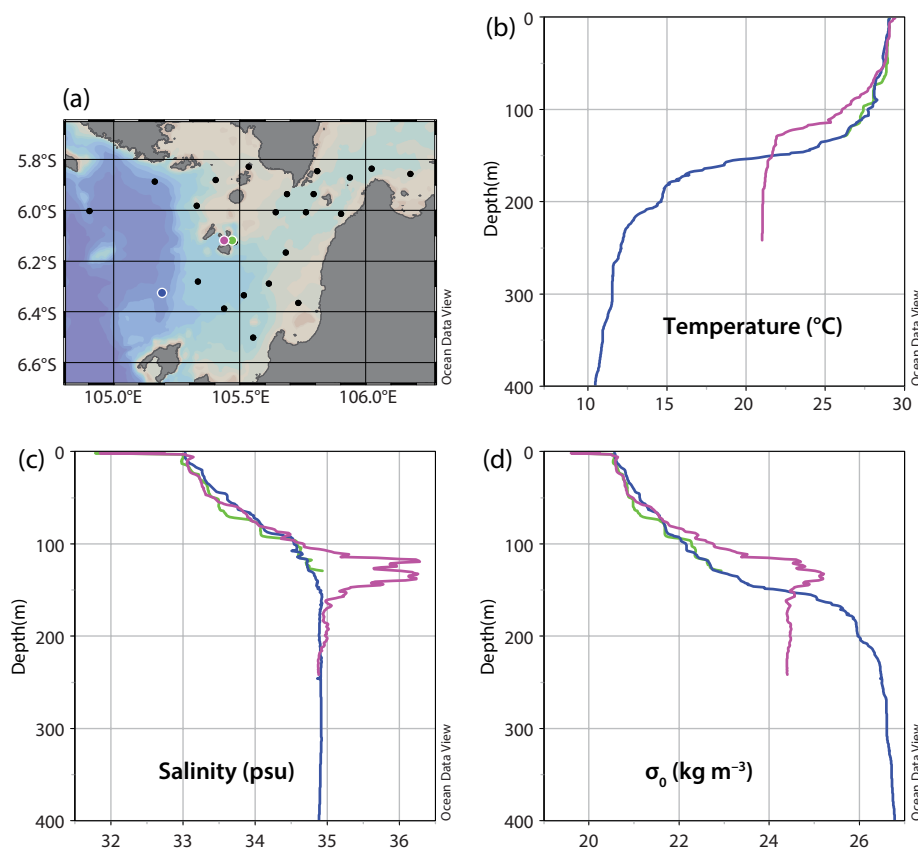Tidal currents in the Sunda Strait are mostly diurnal, with maximum

FIGURE 3. (a) CTD stations taken in November 2008 (dots) at the eastern entrance of the original Krakatau crater (green), in the center of that crater (purple) and in the Indian Ocean (blue). The plots show variability of (b) temperature, (c) salinity, and (d) density anomaly (σ_0). The high-salinity layer (between 120 m and 140 m) recorded in the center of the original Krakatau crater was puzzling.

occurrence at mid-depth. Fortnightly tidal modulation is also clearly observed in the velocity time series, indicating strong tidal mixing in the region. To remove the tidal effects, a two-day Lanczos low-pass filter was applied to every layer (Duchon, 1979). For clarity in presenting the velocity profile shown in Figure 6, a two-week low-pass filter was applied to the velocity. Figure 6b shows averaged zonal wind stress to the north and south of Java, and Figure 6c and d shows the subtidal velocity profile time series derived from the ADCP at Sunda East from November 2008 to October 2009 and Sunda West from November 2008 to July 2009, respectively. The mean and standard deviation as well as the maximum and minimum velocity were calculated based on the two-day low-pass filter (before the two-week low-pass filter was applied). The depth-averaged seasonal mean velocity and its standard deviation from the Sunda West data from November 8, 2008, to March 4, 2009, and from March 5 to July 22, 2009, is 0.0 ± 0.04 m s^{-1} and -0.42 ± 0.06 m s^{-1}, respectively. Meanwhile, the depth-averaged seasonal mean velocity and its standard deviation from Sunda East data from November 8, 2008, to March 4, 2009, and from March 5 to October 20, 2009, is 0.12 ± 0.03 m s^{-1} and -0.34 ± 0.03 m s^{-1}, respectively. The maximum southward velocity is 1.54 m s^{-1}, while the maximum northward velocity is 0.68 m s^{-1}. Negative values denote southward flow toward the Indian Ocean. The apparent intraseasonal and seasonal variability can be seen.

Similar to the Lombok Strait (Susanto et al., 2007), the seasonal reversal of Sunda Strait velocity is caused by Ekman transport and geostrophic transport (east-west pressure gradient) due to the reversal of monsoon winds. The Ekman transport principle says that in the Southern Hemisphere, net water transport/displacement due to wind forcing is 90° to the left of the wind direction (Figure 6a; Pond and Pickard, 1983). Sprintall and Liu (2005) show that Ekman transport drives seasonal variability of
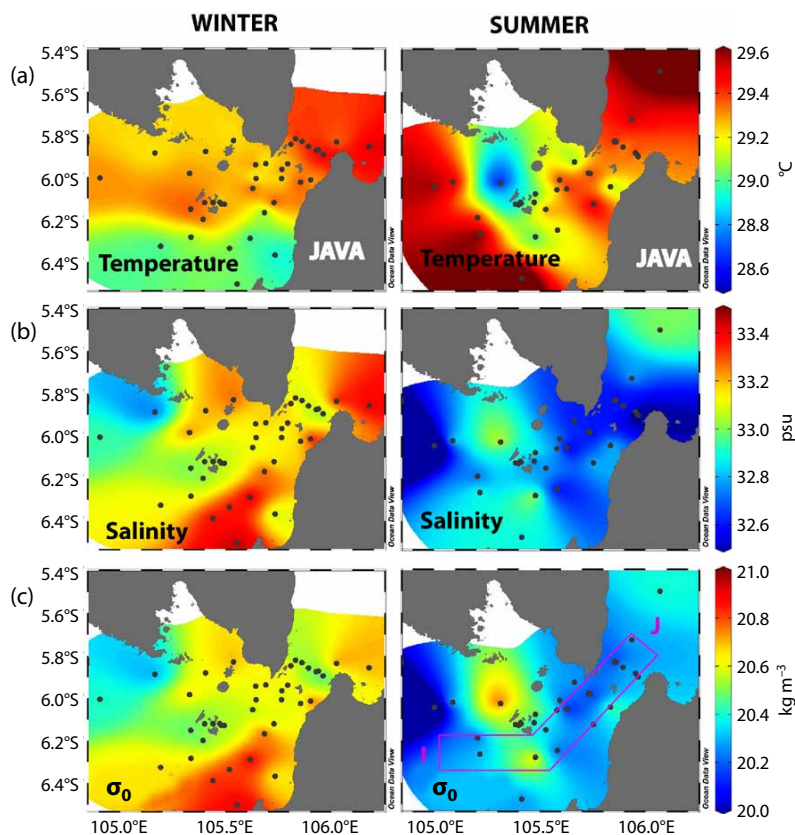

FIGURE 4. Variability of temperature, salinity, and density anomaly (σ_o) in the Sunda Strait during the winter and summer monsoons derived from CTD data (black dots) averaged in the top 20 m. The purple box in the right panel of (c) shows the section from the Indian Ocean side (I) to the Java Sea site (J). Water properties along this section are shown in Figure 5.
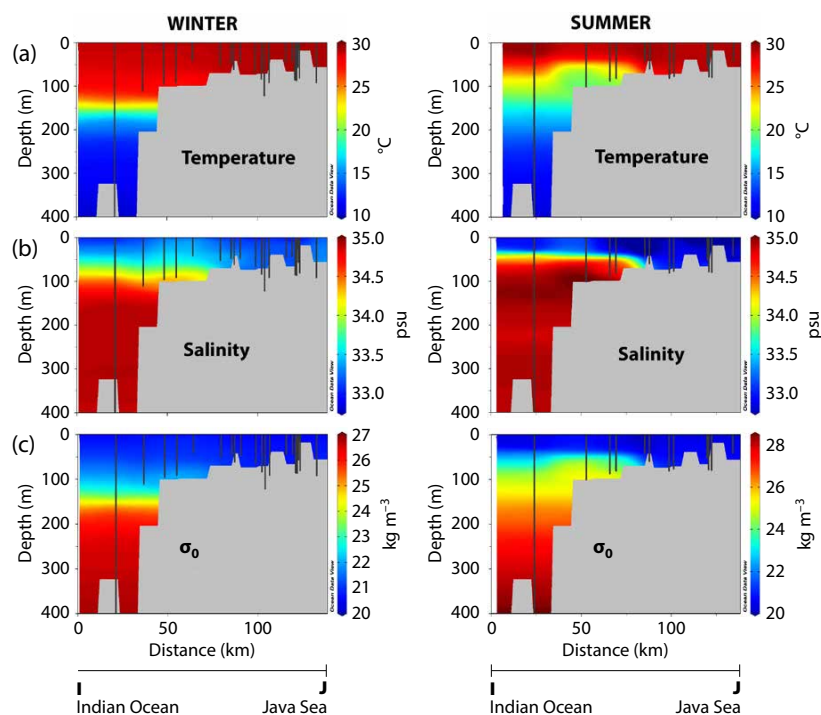

FIGURE 5. Variability of temperature, salinity, and density anomaly (σ_o) with depth along the Sunda Strait section outlined in purple in the right panel of Figure 4c, derived from CTD data collected during the winter and summer monsoons (black vertical lines). The bathymetric cross section is based on the 2 minute x 2 minute gridded GEBCO data set.

the ITF along Nusa Tenggara Island. To enhance the interpretation, zonal wind stress obtained from IFREMER (http://cersat.ifremer.fr) for the regions to the north and south of Java from 12°S to 3°S and 100°E to 115°E is averaged (Figure 6b). The significant correlation value between zonal wind stress and the along-strait velocity at 10 m depth is 0.76 at zero time lag, with a confidence interval exceeding 99% (verified using Monte-Carlo simulations on 1,000 randomized time series; Gentle, 2003). A preliminary estimate of the Sunda Strait transport based on the current velocity is 0.24 ± 0.1 Sv and –0.83 ± 0.2 Sv for the boreal winter and summer monsoon, respectively. As Figure 6b shows, during the boreal winter/northwest monsoon (November to March), the averaged

zonal wind stress to the north and south of Java is positive (eastward), drawing Sunda Strait water northward into the Java Sea. Meanwhile, the eastward zonal wind south of Java (a downwelling-favorable wind) causes waters to accumulate along the island's southern coast and enhances the northward flow in the Sunda Strait from the Indian Ocean into the Java Sea (cyan arrows in Figure 1a,b). At the same time, during this monsoon season, South China Sea water also enters the Java Sea (cyan arrows in Figure 1a,b), which strongly influences the vertical structure of the main ITF from the Pacific Ocean into the Makassar Strait (Gordon et al., 2003, 2012; Qu et al., 2006; Fang et al., 2009, 2010; Tozuka et al., 2009; Susanto et al., 2010, 2012, 2013). Hence, the Sunda Strait conditions increase the complexity of seasonal impacts of the Java Sea flow on the ITF.

Conditions are reversed during the boreal summer/southeast monsoon (May to September). Negative/westward wind stress to the north and south of Java pushes waters from the Java Sea into the Indian Ocean via the Sunda Strait. This condition enhances the upper layer of the Makassar Strait main throughflow, which partially enters the Java Sea and finally flows into the Indian Ocean via the Sunda Strait (purple arrow in Figure 1b). The westward wind stress south of the Java Sea induces seasonal upwelling and results in low sea surface height and low temperature along the southern coasts of Java and Sumatra (Susanto et al., 2001), enhancing the southward flow of waters through the Sunda Strait toward the Indian Ocean. Meanwhile, intrusion of Sunda Strait water with high chlorophyll-*a* concentration into the Indian Ocean can be seen in satellite images of ocean color/chlorophyll-*a* (Susanto and Marra, 2005). It is expected that the southward Sunda Strait flow would be enhanced during El Niño and positive DMI due to strong anomalous easterly winds along the southern coast of Java, reducing sea surface temperature, lowering sea surface height, and
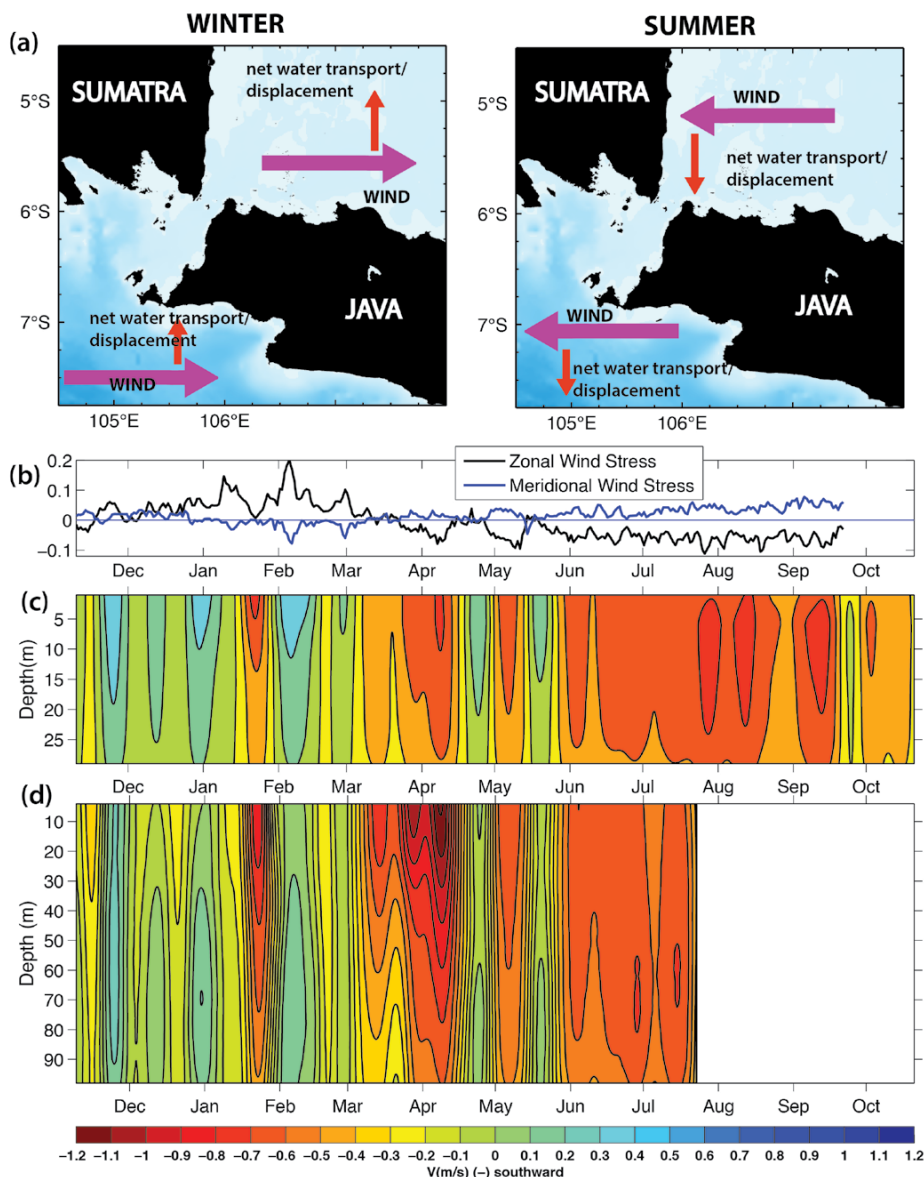

FIGURE 6. (a) Schematic of Ekman transport in the Southern Hemisphere during boreal winter and summer monsoons. Wind directions are indicated by the purple arrows and their net water transport/displacements, which are 90° to the left of wind directions, by the red arrows. (b) Averaged zonal wind stress to the north and south of Java Island from 12°S to 3°S and 100°E to 115°E. (c) Along-strait velocity profile time series in the Sunda Strait based on trawl-resistant, bottom-mounted acoustic Doppler current profiler (ADCP) data collected at Sunda East from November 2008 to October 2009. (d) Similar data as in (c), based on the Sunda West ADCP from November 2008 to July 2009. For clarity in the velocity plots, a two-week low-pass filter has been applied.

enhancing upwelling (Saji et al., 1999; Webster et al., 1999; Susanto et al., 2001, 2006; Susanto and Marra, 2005).

The variability of the zonal wind stress to the north and south of Java controls the variability and direction of Sunda Strait flow. An intermittent southward flow occurred in November 2008 and January 2009 when there was slack (westward) zonal wind stress north and south of Java (Figure 6). During monsoon transitions and early monsoon in April and May as well as September and October, there are northward flows, which may be associated with intrusion of coastally trapped Kelvin waves due to a Wyrtki jet in the equatorial Indian Ocean (Wyrtki, 1973; Qiu et al., 2009; Nagura and McPhaden, 2010). The timing coincides with semi-annual Kelvin waves originating in the tropical Indian Ocean (Arief and Murray, 1996; Sprintall et al., 2000; Potemra et al., 2002; Syamsudin et al., 2004; Iskandar et al., 2005; Drushka et al., 2010; Susanto et al., 2012). Additional data and further analysis, combined with an analytical and numerical approach, are required to explain possible Kelvin wave intrusion into the Sunda Strait.

CONCLUSIONS

Water properties obtained from CTD casts from 2008 to 2015 and current velocities from moorings deployed in the Sunda Strait from 2008 to 2009 indicate that flow in the Sunda Strait is influenced by seasonal reversal of monsoon winds. Northward flow occurs during the boreal winter monsoon (November to March); greater sea surface height along the southern coasts of Sumatra and Java and eastward zonal wind stress draw waters from the Indian Ocean into the Java Sea. Conditions are reversed during the boreal summer monsoon (May to September). The seasonal reversal of flow adds complexity to our understanding of how flow in the Java Sea affects the main ITF in the Makassar Strait before those waters exit into the Indian Ocean via the Lombok Strait, Ombai Strait, and Timor Passage. In phase with the seasonal reversal of

transport of low-salinity water from/to the South China Sea via the Karimata Strait (–2.7 ± 1.1 Sv [boreal winter] and 1.2 ± 0.6 Sv [summer]; Fang et al., 2010; Susanto et al., 2013), the Sunda Strait seasonal reversal low-salinity transport plays a double role (reduces and enhances) the exchange between the Pacific and Indian Oceans. This seasonal reversal of Sunda Strait flow is regionally important. During the boreal winter, low-salinity water entering the Java Sea through the Sunda Strait (0.24 ± 0.1 Sv) and Karimata Strait (2.7 ±1.1 Sv) reduces the main ITF in the Makassar Strait. These lower-salinity and lower-density Java Sea waters force the high-salinity and high-density Pacific waters to flow beneath them. During the boreal summer (May to September) when the flow is reversed, the Sunda Strait itself can contribute volume transport (–0.83 ± 0.2 Sv) by exporting lower-salinity and lower-density water from the Java Sea into the Indian Ocean, enhancing the ITF from the Pacific into the Indian Ocean. Semi-annual northward flow during the monsoon transition may be associated with coastal Kelvin waves that originate in the tropical Indian Ocean, a phenomenon that needs further investigation. ◎

REFERENCES

Aldrian, E., and R.D. Susanto. 2003. Identification of three dominant rainfall regions within Indonesia and their relationship to sea surface temperature. *International Journal of Climatology* 23(12):1,435–1,452, http://dx.doi.org/10.1002/joc.950.

Arief, D., and S. Murray. 1996. Low-frequency fluctuations in the Indonesian throughflow through Lombok Strait. *Journal of Geophysical Research* 101:12,455–12,464, http://dx.doi.org/10.1029/96JC00051.

Bryden, H.L., and S. Imawaki. 2001. Ocean transport of heat. Pp. 455–475 in *Ocean Circulation and Climate*. G.J. Siedler, J. Church, and J. Gould, eds, Academic Press, San Diego, CA.

Drushka, K., J. Sprintall, S.T. Gille, and I. Brodjonegoro. 2010. Vertical structure of Kelvin waves in the Indonesian throughflow exit passages. *Journal of Physical Oceanography* 40:1,965–1,987, http://dx.doi.org/10.1175/2010JPO4380.1.

Duchon, C. 1979. Lanczos filtering in one and two dimensions. *Journal of Applied Meteorology* 18:1,016–1,022, http://dx.doi.org/10.1175/1520-0450(1979)018<1016:LFIOAT>2.0.CO;2.

Fang, G., R.D. Susanto, I. Soesilo, Q. Zheng, F. Qiao, and W. Zexun. 2005. A note on the South China Sea shallow interocean circulation. *Advances in Atmospheric Sciences* 22:946–954, http://dx.doi.org/10.1007/BF02918693.

Fang, G., R.D. Susanto, S. Wirasantosa, F. Qiao, A. Supangat, B. Fan, Z. Wei, B. Sulistiyo, and S. Li. 2010. Volume, heat, and freshwater transports from the South China Sea to Indonesian seas in the boreal winter of 2007–2008. *Journal of Geophysical Research* 115, C12020, http://dx.doi.org/10.1029/2010JC006225.

Fang, G., Y. Wang, Z. Wei, Y. Fang, F. Qiao, and X. Hu. 2009. Interocean circulation and heat and freshwater budgets of the South China Sea based on a numerical model. *Dynamics of Atmospheres and Oceans* 47:55–72, http://dx.doi.org/10.1016/j.dynatmoce.2008.09.003.

Gentle, J.E. 2003. *Random Number Generation and Monte Carlo Methods,* 2nd ed. Springer, New York.

Godfrey, J.S. 1996. The effect of the Indonesian throughflow on ocean circulation and heat exchange with the atmosphere: A review. *Journal of Geophysical Research* 101(C5):12,217–12,237, http://dx.doi.org/10.1029/95JC03860.

Gordon, A.L., B.A. Huber, E.J. Metzger, R.D. Susanto, H.E. Hurlburt, and T.R. Adi. 2012. South China Sea throughflow impact on the Indonesian throughflow. *Geophysical Research Letters* 33(11), http://dx.doi.org/10.1029/2012GL052021.

Gordon, A., J. Sprintall, H. van Aken, R.D. Susanto, S. Wijffels, R. Molcard, A. Ffield, and W. Pranowo. 2010. The Indonesian throughflow during 2004–2006 as observed by the INSTANT program. *Dynamics of Atmospheres and Oceans* 50(2):113–114, http://dx.doi.org/10.1016/j.dynatmoce.2009.12.002.

Gordon, A., R.D. Susanto, A. Ffield, B. Huber, W. Pranowo, and S. Wirasantosa. 2008. Makassar Strait throughflow 2004 to 2006. *Geophysical Research Letters* 35, L24605, http://dx.doi.org/10.1029/2008GL036372.

Gordon, A.L., R.D. Susanto, and K. Vranes. 2003. Cool Indonesian throughflow as a consequence of restricted surface layer flow. *Nature* 425:824–828, http://dx.doi.org/10.1038/nature02038.

Iskandar, I., W. Mardiansyah, Y. Masumoto, and T. Yamagata. 2005. Intraseasonal Kelvin waves along the southern coast of Sumatra and Java. *Journal of Geophysical Research* 110, C04013, http://dx.doi.org/10.1029/2004JC002508.

Lee, S.-K., W. Park, M.O. Baringer, A.L. Gordon, B. Huber, and Y. Liu. 2015. Pacific origin of the abrupt increase in Indian Ocean heat content during the warming hiatus. *Nature Geoscience* 8:445–449, http://dx.doi.org/10.1038/ngeo2438.

Lee, T., I. Fukumori, D. Menemenlis, Z. Xing, and L.L. Fu. 2002. Effects of the Indonesian throughflow on the Pacific and Indian Oceans. *Journal of Physical Oceanography* 32:1,404–1,429, http://dx.doi.org/10.1175/1520-0485(2002)032<1404:EOTITO>2.0.CO;2.

Lee, T., and M.J. McPhaden. 2008. Decadal phase changes in large-scale sea level and winds in the Indo-Pacific region at the end of the 20th century. *Geophysical Research Letters* 35, L01605, http://dx.doi.org/10.1029/2007GL032419.

Madden, R.A., and P.R. Julian. 1994. Observations of the 40–50-day tropical oscillation: A review. *Monthly Weather Review* 122:814–837, http://dx.doi.org/10.1175/1520-0493(1994)122<0814:OOTDTO>2.0.CO;2.

Murray, S.P., and D. Arief. 1988. Throughflow into the Indian Ocean through the Lombok Strait, January 1985–January 1986. *Nature* 333:444–447, http://dx.doi.org/10.1038/333444a0.

Nagura, M., and M.J. McPhaden. 2010. Wyrtki jet dynamics: Seasonal variability. *Journal of Geophysical Research* 115, C07009, http://dx.doi.org/10.1029/2009JC005922.

Pond, S., and G.L. Pickard. 1983. *Introductory Dynamical Oceanography,* 2nd *ed.* Butterworth-Heinemann Ltd., Oxford.

Potemra, J.T., S.L. Hautala, J. Sprintall, and W. Pandoe. 2002. Interaction between the Indonesian Seas and the Indian Ocean in observations and numerical models. *Journal of Physical Oceanography* 32:1,838–1,854, http://dx.doi.org/10.1175/1520-0485(2002)032<1838:IBTISA>2.0.CO;2.

Reed, C. 2015. Tracking the missing heat from the global warming hiatus. *Eos,* 96, http://dx.doi.org/10.1029/2015EO029947. Published on May 21, 2015.

Qiu, Y., L. Li, and W. Yu. 2009. Behavior of the Wyrtki jet observed with surface drifting buoys and satellite altimeter. *Geophysical Research Letters* 36, L18607, http://dx.doi.org/10.1029/2009GL039120.

Qu, T., D. Yan, and H. Sasaki. 2006. South China Sea throughflow: A heat and freshwater conveyor. *Geophysical Research Letters* 33, L23617, http://dx.doi.org/10.1029/2006GL028350.

Saji, N.H., B.N. Goswami, P.N. Vinayachandran, and T. Yamagata. 1999. A dipole mode in the tropical Indian Ocean. *Nature* 401:360–363, http://dx.doi.org/10.1038/43854.

Schneider, N. 1998. The Indonesian throughflow and the global climate system. *Journal of Climate* 11:676–689, http://dx.doi.org/10.1175/1520-0442(1998)011<0676:TITATG>2.0.CO;2.

Shinoda, T., W. Han, E.J. Metzger, and H. Hurlburt. 2012. Seasonal variation of the Indonesian throughflow in Makassar Strait. *Journal of Physical Oceanography* 42:1,099–1,123, http://dx.doi.org/10.1175/JPO-D-11-0120.1.

Simkin, T., and R.S. Fiske. 1983. *Krakatau, 1883: The Volcanic Eruption and Its Effects.* Smithsonian Institution Press, Washington, DC, 464 pp.

Sprintall, J., J. Chong, F. Syamsudin, W. Morawitz, S. Hautala, N. Bray, and S. Wijffels. 1999. Dynamics of the South Java current in the Indo-Australian Basin. *Geophysical Research Letters* 26:2,493–2,496, http://dx.doi.org/10.1029/1999GL002320.

Sprintall, J., A.L. Gordon, A. Koch-Larrouy, T. Lee, J.T. Potemra, K. Pujiana, and S.E. Wijffels. 2014. The Indonesian seas and their role in the coupled ocean-climate system. *Nature Geoscience* 7(7):487–492, http://dx.doi.org/10.1038/ngeo2188.

Sprintall, J., A.L. Gordon, R. Murtugudde, and R.D. Susanto. 2000. A semiannual Indian Ocean forced Kelvin wave observed in the Indonesian seas in May 1997. *Journal of Geophysical Research* 105:17,217–17,230, http://dx.doi.org/10.1029/2000JC900065.

Sprintall, J., and W.T. Liu. 2005. Ekman mass and heat transport in the Indonesian Seas. *Oceanography* 18(4):88–97, http://dx.doi.org/10.5670/oceanog.2005.09.

Sprintall, J., and A. Revelard. 2014. The Indonesian throughflow response to Indo-Pacific climate variability. *Journal of Geophysical Research* 119:1,161–1,175, http://dx.doi.org/10.1002/2013JC009533.

Sprintall, J., S.E. Wijffels, R. Molcard, and I. Jaya. 2009. Direct estimates of the Indonesian throughflow entering the Indian Ocean: 2004–2006. *Journal of Geophysical Research* 114, C07001, http://dx.doi.org/10.1029/2008JC005257.

Susanto, R.D., G. Fang, I. Soesilo, Q. Zheng, F. Qiao, Z. Wei, and B. Sulistyo. 2010. New surveys of a branch of the Indonesian throughflow. *Eos, Transactions American Geophysical Union* 91(30):261–263, http://dx.doi.org/10.1029/2010EO300002.

Susanto, R.D., A. Ffield, A.L. Gordon, and T.R. Adi. 2012. Variability of Indonesian throughflow within Makassar Strait throughflow: 2004 to 2009. *Geophysical Research Letters* 117, C09013, http://dx.doi.org/10.1029/2012JC008096.

Susanto, R.D., A.L. Gordon, and J. Sprintall. 2007. Observations and proxies of the surface layer throughflow in Lombok Strait. *Journal of Geophysical Research* 112, C03S92, http://dx.doi.org/10.1029/2006JC003790.

Susanto, R.D., A.L. Gordon, J. Sprintall, and B. Herunadi. 2000. Intraseasonal variability and tides in Makassar Strait. *Geophysical Research Letters* 27:1,499–1,502, http://dx.doi.org/10.1029/2000gl011414.

Susanto, R.D., A.L. Gordon, and Q. Zheng. 2001. Upwelling along the coasts of Java and Sumatra and its relation to ENSO. *Geophysical Research Letters* 28:1,599–1,602, http://dx.doi.org/10.1029/2000GL011844.

Susanto, R.D., and J. Marra. 2005. Effect of the 1997/98 El Niño on chlorophyll *a* variability along the southern coasts of Java and Sumatra. *Oceanography* 18(4)124–127, http://dx.doi.org/10.5670/oceanog.2005.13.

Susanto, R.D., T. Moore II, and J. Marra. 2006. An ocean color variability in the Indonesian Seas during the SeaWifs era. *Geochemistry Geophysics Geosystems* 7, Q05021, http://dx.doi.org/10.1029/2005GC001009.

Susanto, R.D., and Y.T. Song. 2015. Indonesian throughflow proxy from satellite altimeters and gravimeters *Journal of Geophysical Research* 120:2,844–2,855, http://dx.doi.org/10.1002/2014JC010382.

Susanto, R.D, Z. Wei, T.R. Adi, B. Fan, S. Li, and G. Fang. 2013. Observations of the Karimata Strait throughflow from December 2007 to November 2008. *Acta Oceanologica Sinica* 32(5):1–6, http://dx.doi.org/10.1007/s13131-013-0307-3.

Syamsudin, F., A. Kaneko, and D.B. Haidvogel. 2004. Numerical and observational estimates of Indian Ocean Kelvin intrusion into Lombok Strait. *Geophysical Research Letters* 32, L24307, http://dx.doi.org/10.1029/2004GL021227.

Tokinaga, H., S.-P. Xie, A. Timmermann, S. McGregor, T. Ogata, H. Kubota, and Y.M. Okumura. 2012. Regional patterns of tropical Indo-Pacific Climate change: Evidence of the Walker Circulation weakening. *Journal of Climate,* http://dx.doi.org/10.1175/JCLI-D-11-00263.1.

Tozuka, T., T. Qu, Y. Masumoto, and T. Yamagata. 2009. Impacts of the South China Sea throughflow on seasonal and interannual variations of the Indonesian Throughflow. *Dynamics of Atmospheres and Oceans* 47:73–85, http://dx.doi.org/10.1016/j.dynatmoce.2008.09.001.

van Aken, H.M., I.S. Brodjonegoro, and I. Jaya. 2009. The deep water motion through the Lifamatola Passage and its contribution to the Indonesian throughflow. *Deep-Sea Research Part I* 56:1,203–1,216, http://dx.doi.org/10.1016/j.dsr.2009.02.001.

Webster, P.J., A.M. Moore, J.P. Loschnigg, and R.R. Leben. 1999. Coupled ocean-atmosphere dynamics in the Indian Ocean during 1997–98. *Nature* 401:356–360, http://dx.doi.org/10.1038/43848.

Wei, Z.X., G.H. Fang, R.D. Susanto, T.R. Adi, B. Fan, A. Setiawan, S.J. Li, Y.G. Wang, and X.M. Gao. 2015. Tidal elevation, current and energy flux in the area between the South China Sea and Java Sea. *Ocean Science* 12:2,831–2,861, http://dx.doi.org/10.5194/osd-12-2831-2015.

Wyrtki, K. 1973. An equatorial jet in the Indian Ocean. *Science* 181:262–264, http://dx.doi.org/10.1126/science.181.4096.262.

Wyrtki, K. 1987. Indonesian throughflow and the associated pressure gradient. *Journal of Geophysical Research* 92:12,941–12,946, http://dx.doi.org/10.1029/JC092iC12p12941.

AUTHORS

R. Dwi Susanto (dwisusa@umd.edu) is Senior Research Scientist, Department of Atmospheric and Oceanic Science, University of Maryland, College Park, MD, USA, and Center for Oceanography and Marine Technology, Surya University, Tangerang, Indonesia. **Zexun Wei** is Research Scientist, Laboratory for Regional Oceanography and Numerical Modeling, Qingdao National Laboratory for Marine Science and Technology, Qingdao, China, and The First Institute Oceanography, State Oceanic Administration, Qingdao, China. **T. Rameyo Adi** is Research Scientist, Agency for Marine and Fisheries Research and Development, Jakarta, Indonesia. **Quanan Zheng** is Senior Research Scientist, Department of Atmospheric and Oceanic Science, University of Maryland, College Park, MD, USA. **Guohong Fang** is Research Scientist, Laboratory for Regional Oceanography and Numerical Modeling, Qingdao National Laboratory for Marine Science and Technology, Qingdao, China, and The First Institute Oceanography, State Oceanic Administration, Qingdao, China. **Bin Fan** is Research Scientist, The First Institute Oceanography, State Oceanic Administration, Qingdao, China. **Agus Supangat** is Professor, Climate Change Center, Bandung Institute of Technology, Bandung, Indonesia. **Teguh Agustiadi** is Researcher, Agency for Marine and Fisheries Research and Development, Jakarta, Indonesia. **Shujiang Li** is Research Scientist, Laboratory for Regional Oceanography and Numerical Modeling, Qingdao National Laboratory for Marine Science and Technology, Qingdao, China, and The First Institute Oceanography, State Oceanic Administration, Qingdao, China. **Mukti Trenggono** is Researcher, Agency for Marine and Fisheries Research and Development, Jakarta, Indonesia. **Agus Setiawan** is Researcher, Agency for Marine and Fisheries Research and Development, Jakarta, Indonesia.